Supporting Information for

Decarbonylation of Ethanol to Methane, Carbon Monoxide and Hydrogen by a [PNP]Ir Complex

Jonathan G. Melnick, Alexander T. Radosevich, Dino Villagrán and Daniel G. Nocera*

Department of Chemistry, 6-355, Massachusetts Institute of Technology, 77 Massachusetts Avenue, Cambridge, Massachusetts 02139-4307

Experimental Methods

General Considerations. All manipulations were carried out in oven-dried glassware under an inert atmosphere provided either by a N_2-filled glovebox or by using standard Schlenk techniques. All reaction solvents were reagent grade (Aldrich) or better and were dried and degassed by standard methods.[1] $[PNP^{Pr^i}]Ir(H)_2$[2] and 2,4,6-Me_3-C_6H_2-N_3 $(MesN_3)$[3] were prepared according to the literature methods. Norbornylene (NBE) was purchased from Aldrich and used without further purification. $CDCl_3$ and C_6D_6 were purchased from Cambridge Isotope Laboratories and stored over activated 4 Å MS in the glovebox prior to use.

^1H, ^{13}C, and ^{31}P NMR spectra were acquired on a Bruker DRX 400 MHz spectrometer in the specified solvent in sealable J. Young NMR tubes. ^1H and ^{13}C NMR spectra were calibrated against the residual protio-solvent resonances (benzene δ 7.16); ^{31}P NMR spectra were referenced externally to H_3PO_4 (δ 0 ppm). Infrared spectra were acquired on a Perkin-Elmer Model 2000 FT-IR spectrophotometer in a potassium bromide matrix. UV-vis spectra were recorded at room temperature in quartz cuvettes on a Varian Cary 5000 UV-vis-NIR spectrophotometer. Photochemical reactions were performed using a 1000 W high pressure Hg/Xe arc lamp (Oriel). The beam was passed through a water-jacketed filter holder containing appropriate long pass filters, an iris, and collimating lens. High resolution electrospray ionization mass spectrometry was performed in the MIT Department of Chemistry Instrument Facility. Mass spectrometric analysis of evolved methane and hydrogen was performed using an Agilent Technologies 5975C mass selective detector operating in electron impact ionization mode. Gas chromatography quantification of hydrogen and methane was performed o an HP 6890 series GC equipped with a 50 m × 0.530 mm, 25 μm, HP Mole Sieve column and a thermal conductivity detector (TCD). An injection temperature of 150°C, oven temperature of 200°C, and detector temperature of 250°C were used with a flow rate of the carrier gas, N_2, at 8 psi or 5 mL/min. Elemental analysis was performed by Midwest Microlabs (Indianapolis, IN).

Synthesis of *trans*-$[PNP^{Pr^i}]Ir(H)(Me)(CO)$. Three synthetic routes afforded *trans*-$[PNP^{Pr^i}]Ir(H)(Me)(CO)$: (a) In a 100 mL Schlenk flask equipped with a magnetic stirbar, a mixture of $[PNP^{Pr^i}]Ir(H)_2$ (100 mg, 0.16 mmol) and NBE (100 mg, 1.06 mmol) was treated with ca. 40 mL EtOH. The mixture slowly dissolves over the course of 1 h, and was stirred at room temperature for 1 d over which time the solution turns yellow. The solvent was removed *in vacuo* to give $[PNP^{Pr^i}]Ir(H)(Me)(CO)$ as a yellow solid in a yield of 85 mg (80%). Crystals suitable for X-ray diffraction were obtained by cooling a saturated solution of $[PNP^{Pr^i}]Ir(H)(Me)(CO)$ in Et_2O to –40 °C. (b) In a 100 mL Schlenk flask equipped with a magnetic stirbar, $[PNP^{Pr^i}]Ir(N_2)$ (20 mg, 0.031 mmol) was refluxed in EtOH for 1 d. The solvent

[1] Armarego, W. L. F.; Perrin, D. D. *Purification of Laboratory Chemicals,* 4th ed.; Butterworth–Heinmann: Oxford, 1996.
[2] Fan, L.; Parkin, S.; Ozerov, O. V. *J. Am. Chem. Soc.* **2005**, *127*, 16772-16773.
[3] Ranu, B. C.; Sarkar, A.; Chakraborty, R. *J. Org. Chem.* **1994**, *59*, 4114-4116.

was removed *in vacuo* to give [PNP$^{Pr^i}$]Ir(H)(Me)(CO) as a yellow solid. (c) In a 100 mL Schlenk flask equipped with a magnetic stirbar, a mixture of [PNP$^{Pr^i}$]Ir(H)$_2$ (20 mg, 0.03 mmol) was treated with ca. 5 mL acetaldehyde. The solution was stirred for 1 d at room temperature over which time the color of solution changed from red to yellow. The solvent was removed *in vacuo* and product formation determined by ^{1}H NMR.

^{1}H NMR (C$_6$D$_6$): 7.70 (d, 2H, ^{3}J$_{H-H}$ = 8.8 Hz, Ar-*H*), 6.91 (s, 2H, Ar-*H*), 6.71 (d, 2H, ^{3}J$_{H-H}$ = 8.8 Hz, Ar-*H*), 2.51 (br m, 2H, C*H*Me$_2$), 2.19 (s, 6H, Ar-C*H*$_3$), 2.02 (br m, 2H, C*H*Me$_2$), 1.32 - 0.92 (m, 24H, CH*Me*$_2$), 0.58 (br, 3H, Ir-C*H*$_3$), −8.22 (t, 1H, ^{2}J$_{P-H}$ = 16.0 Hz, Ir-*H*). ^{13}C{^{1}H} NMR (C$_6$D$_6$): 160.4 (t, 1C, ^{2}J$_{P-C}$ = 9.6 Hz, Ir-*C*O), 131.7(s, 2C, (*Ar*PPr^i$_2$)$_2$N), 131.6(s, 2C, (*Ar*PPr^i$_2$)$_2$N), 124.8 (s, 2C, (*Ar*PPr^i$_2$)$_2$N), 123.7(s, 2C, (*Ar*PPr^i$_2$)$_2$N), 123.5(s, 2C, (*Ar*PPr^i$_2$)$_2$N), 117.1(t, 2C, ^{1}J$_{P-C}$ = 5.3 Hz (MeC$_5$H$_3$*C*PPr^i$_2$)$_2$N), 27.4(t, 2C, ^{1}J$_{P-C}$ = 17.9 Hz, *C*HMe$_2$), 26.6(t, 2C, ^{1}J$_{P-C}$ = 15.3 Hz, *C*HMe$_2$), 20.9(s, 2C, CH*Me*$_2$), 20.5(s, 2C, CH*Me*$_2$), 19.6 (s, 2C, Ar-*C*H$_3$), 18.6(s, 2C, CH*Me*$_2$), 18.4(s, 2C, CH*Me*$_2$), −26.9(t, 1C, ^{2}J$_{P-C}$ = 5.8 Hz, Ir-*C*H$_3$). ^{31}P{^{1}H} NMR (C$_6$D$_6$): 40.7 (s).

IR Data (KBr pellet, cm^{-1}) 2960(m), 2922(m), 2870(m), 2361(s), 2342(m), 2171(w), 1987(vs, CO), 1932(s), 1595(m), 1458(vs), 1388(w), 1363(w), 1316(s), 1290(w), 1257(w), 1240(w), 1210(w), 1146(w), 1095(w), 1062(w), 1029(w), 928(w), 914(w), 883(m), 828(w), 804(s), 728(w), 703(w), 668(m), 617(w), 588(w), 570(w), 554(w), 534(w), 515(w), 501(w), 472(w), 449(w), 419(w).

Analysis Calcd. for [PNP$^{Pr^i}$]Ir(H)(Me)(CO): C, 50.6%; H, 6.7%; N, 2.1%. Found: C, 50.3%; H, 6.5%; N, 2.4%.

Mass spectrum: 665.2 {M}$^+$, 650.2 {M − CH$_4$ + 1}$^+$.

Synthesis of *trans*-[PNP$^{Pr^i}$]Ir(H)(Et)(CO). In a 100 mL Schlenk flask equipped with a magnetic stirbar, a mixture of [PNP$^{Pr^i}$]Ir(H)$_2$ (160 mg, 0.25 mmol) and NBE (140 mg, 1.49 mmol) was treated with ca. 20 mL *n*-PrOH. The mixture slowly dissolved over the course of 1 h, and was stirred at room temperature for 1 d over which time the solution turned yellow. The solvent was removed *in vacuo* to give [PNP$^{Pr^i}$]Ir(H)(Et)(CO) as a yellow solid. Yield 130 mg, 75%. Crystals suitable for X-ray diffraction were obtained by cooling a saturated solution of [PNP$^{Pr^i}$]Ir(H)(Et)(CO) in Et$_2$O to −40°C.

^{1}H NMR (C$_6$D$_6$): 7.69 (d, 2H, ^{3}J$_{H-H}$ = 8.4 Hz, Ar-*H*), 6.90 (s, 2H, Ar-*H*), 6.72 (d, 2H, ^{3}J$_{H-H}$ = 8.4 Hz, Ar-*H*), 2.60 (m, 2H, C*H*Me$_2$), 2.19 (s, 6H, Ar-C*H*$_3$), 1.97 (m, 2H, C*H*Me$_2$), 1.95 (t, 2H, ^{3}J$_{H-H}$ = 7.0 Hz, IrCH$_2$C*H$_3$*), 1.57 (m, 2H, ^{3}J$_{H-H}$ = 7.0 Hz, IrC*H$_2$*CH$_3$), 1.32 - 1.14 (m, 18H, CH*Me*$_2$), 0.92 (m, 6H, CH*Me*$_2$), −8.88 (t, 1H, ^{2}J$_{P-H}$ = 17.0 Hz, Ir-*H*). ^{31}P{^{1}H} NMR (C$_6$D$_6$): 39.6 (s).

IR Data (KBr pellet, cm^{-1}) 2929(m), 2362(m), 2341(m), 2171(w), 1973(vs, CO), 1931(m), 1458(vs), 1378 (w), 1313(s), 1257(w), 1210(w), 1148(w), 1067(w), 1029(w), 929(w), 881(w), 801(m), 729(w), 703(w), 668(w), 655(m), 636(m), 590(w), 572(w), 557(w), 517(m), 473(w), 419(w).

Analysis Calcd. for $[PNP^{Pr^i}]Ir(H)(Et)(CO)$: C, 51.3%; H, 6.8%; N, 2.1%. Found: C, 51.3%; H, 6.9%; N, 2.2%.

Mass spectrum: 680.3 $\{M+1\}^+$, 650.2 $\{M-C_2H_6+1\}^+$

Synthesis of $[PNP^{Pr^i}]Ir(CO)$: From *trans*-$[PNP^{Pr^i}]Ir(H)(Me)(CO)$. In a J. Young NMR tube, *trans*-$[PNP^{Pr^i}]Ir(H)(Me)(CO)$ in C_6D_6 with 1 μL mesitylene as an internal standard was photolyzed ($\lambda_{exc} \geq 338$ nm) for 16 h. The resulting product was determined by ^{1}H NMR to be 98.5% formation of $[PNP^{Pr^i}]Ir(CO)^4$ accompanied by formation of CH_4 ($\delta = 0.16$ ppm).

From trans-$[PNPPri]Ir(H)(Et)(CO)$. In a J. Young NMR tube, *trans*-$[PNP^{Pr^i}]Ir(H)(Me)(CO)$ in C_6D_6 with 1 μL mesitylene as an internal standard was photolyzed ($\lambda_{exc} \geq 338$ nm) with for 16 h. The resulting product was determined by ^{1}H NMR to be 99.3% formation of $[PNP^{Pr^i}]Ir(CO)$ accompanied by formation of C_2H_6 ($\delta = 0.80$ ppm).

Synthesis of $[PNP^{Pr^i}]IrN_2$. A solution of $[PNP^{Pr^i}]Ir(H)_2$ (721 mg, 1.15 mmol) in ~25 mL cyclohexane was treated with $MesN_3$ (185 mg, 1.15 mmol) and stirred at room temperature for 16 h over which time the solution turned from red to dark green. The solvent was removed *in vacuo* initially at room temperature followed by heating at 115 ºC. The dark green powder was isolated to yield 475 mg (63% yield). Crystals of the composition $[PNP^{Pr^i}]Ir(N_2) \cdot MesNH_2$ were obtained from slow evaporation of a C_6H_6 solution of $[PNP^{Pr^i}]Ir(N_2)$ and $MesNH_2$ prior to heating the reaction mixture *in vacuo*. Characterization of $[PNP^{Pr^i}]Ir(N_2)$ has been previously reported.[5]

Conversion of *trans*-$[PNP^{Pr^i}]Ir(H)(Me)(CO)$ to $[PNP^{Pr^i}]Ir(CO)$ under N_2. A stock solution of *trans*-$[PNP^{Pr^i}]Ir(H)(Me)(CO)$ (2 mg, 0.003 mmol) in 20 mL of C_6H_6 (0.15 mM solution) was prepared. 4 mL of the stock solution was added to a high-vacuum Starna cell and photolyzed ($\lambda_{exc} \geq 338$ nm) over 6 min and spectra were recorded in 30 s intervals.
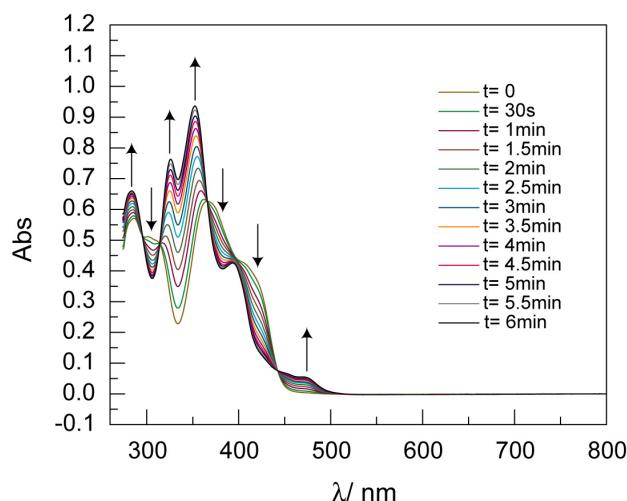
Figure S1. UV-vis trace of photolysis ($\lambda_{exc} \geq 338$ nm) of *trans*-$[PNP^{Pr^i}]Ir(H)(Me)(CO)$ in 30 s increments under 1 atm N_2.

4   Whited, M. T.; Grubbs, R. H. *J. Am. Chem. Soc.* **2008**, *130*, 5874-5875.
5   Whited, M. T.; Grubbs, R. H. *J. Am. Chem. Soc.* **2008**, *130*, 16476-16477.

Photolysis of [PNP$^{Pr^i}$]IrN$_2$ for GC-MS Experiments. Photolysis experiments for GC-MS were carried out in a 2-stopcock reactor custom made by James Glass of Hanover, Massachusetts (Figure S5). [PNP$^{Pr^i}$]Ir(N$_2$) (50 mg, 0.076 mmol) was treated with 5 mL of EtOH (or EtOD) and degassed by three freeze-pump-thaw cycles. The solution was photolyzed for 1 d. The sample was frozen with N$_2(\ell)$ and was rapidly warmed by immersion in water. The evolved gases were fed into the mass spectrometer for real-time analysis with helium used as a carrier gas.
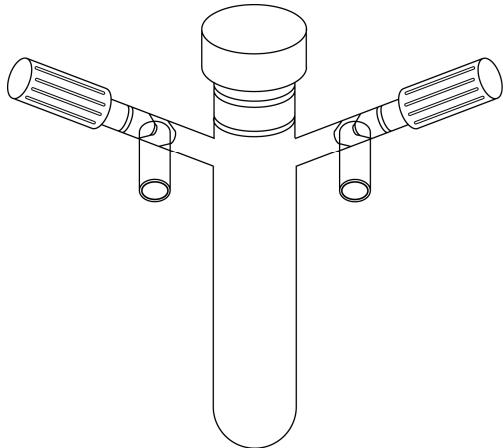

Figure S2. Custom made 2-stopcock reactor used for the GC-MS Experiments of the photolysis of [PNP$^{Pr^i}$]Ir(N$_2$) in EtOH or EtOD.
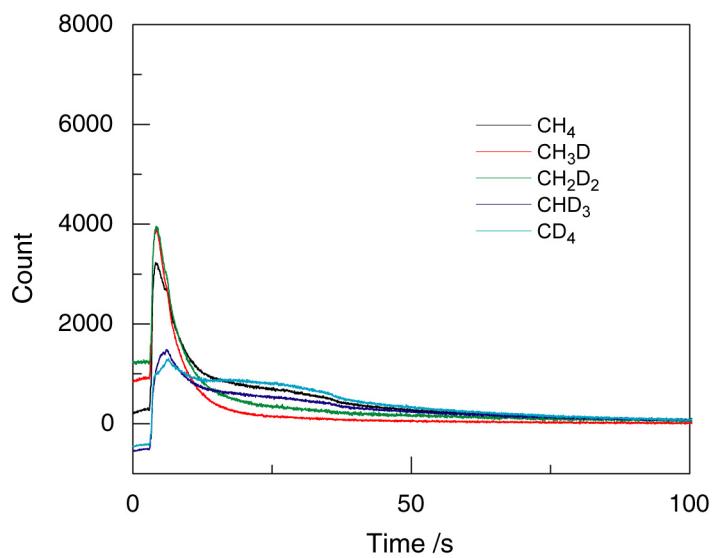
Figure S3. GC-MS of the head space of photolysis of [PNP$^{Pr^i}$]Ir(N$_2$) in EtOD.

Table S2. Percent composition of CH_xD_{4-x} from the GC-MS of the head space of photolysis of $[PNP^{Pr^i}]Ir(N_2)$ in EtOH

	CH_4	CH_3D	CH_2D_2	CHD_3	CD_4	Total count
5 sec	23.9%	27.3%	28.9%	11.1%	8.8%	12401
10 sec	24.9%	18.1%	22.9%	16.2%	17.9%	5404
15 sec	25.7%	11.6%	18.9%	19.1%	24.8%	3431
20 sec	26.7%	7.7%	15.7%	20.3%	29.6%	2861
25 sec	27.5%	5.9%	12.4%	21.2%	33.0%	2487
30 sec	26.8%	5.6%	13.3%	21.3%	32.9%	2272
35 sec	26.6%	5.2%	13.2%	21.3%	33.7%	1888
40 sec	25.8%	6.3%	15.0%	22.1%	30.8%	1451
45 sec	26.7%	4.9%	13.3%	23.8%	31.4%	1212
50 sec	26.0%	5.4%	14.7%	22.0%	31.9%	1025

Photolysis of $[PNP^{Pr^i}]Ir(N_2)$ in EtOH for GC. In a chemglass ampoule. $[PNP^{Pr^i}]Ir(N_2)$ (17 mg, 0.026 mmol) in 5 mL EtOH was photolyzed for 1 d. A sample volume of 20 μL of the headspace was injected into the GC. Under the conditions of the experiments, H_2 has a retention time of 1.11 min. and CH_4 has retention time of 1.27 min (Figure S7). Quantification was performed by integrating the peak corresponding to each evolved gas and fitting it to a standard calibration curve for H_2 or CH_4, which gave a 79% yield of H_2 and a 94% yield of CH_4.
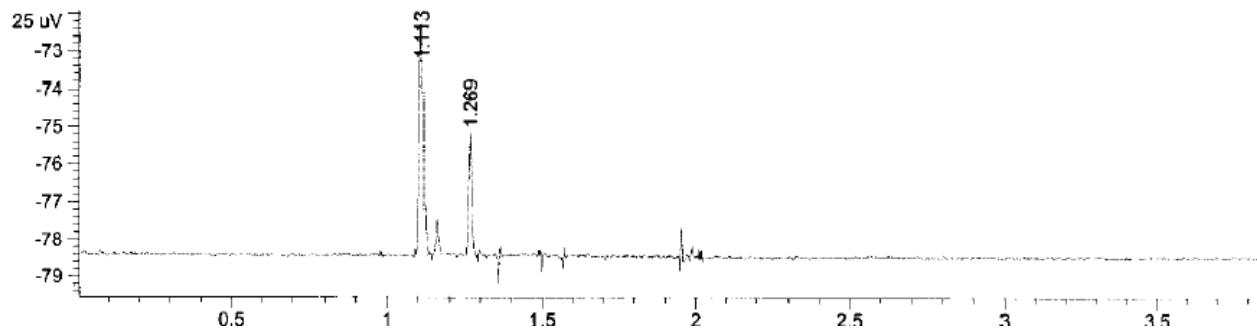
Figure S4. GC of the headspace of the photolysis of $[PNP^{Pr^i}]Ir(N_2)$ in EtOH for the quantification of evolved H_2 and CH_4.

Treatment of $[PNP^{Pr^i}]Ir(H)_2$ with HC(O)Me for quantification of H_2 by GC. In a chemglass ampoule, $[PNP^{Pr^i}]Ir(H)_2$ (40 mg, 0.064 mmol) was treated with 5 mL acetaldehyde. An immediate color change from red to yellow/ orange and vigorous gas evolution is observed. The solution was stirred at room temperature for 30 min. and the headspace was sampled by GC. Under the conditions of the experiments, H_2 has a retention time of 1.11 min (Figure S8). Quantification was performed by integrating the peak corresponding to each evolved gas and fitting it to a standard calibration curve for H_2 which gave a 71% yield of H_2
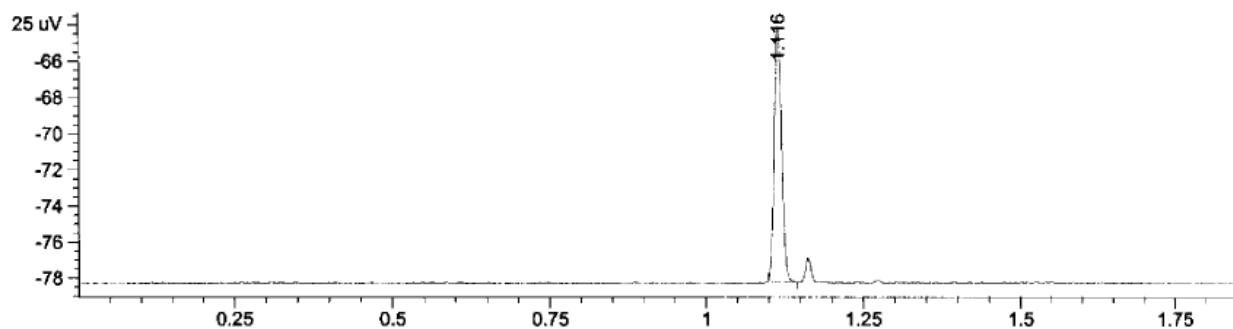
Figure S5. GC of the headspace of the treatment of [PNP$^{Pr^i}$]Ir(H)$_2$ with acetaldehyde for the quantification of evolved H$_2$.

X-ray Crystallographic Details. Single crystals were immersed in a drop of Paratone N oil on a clean microscope slide, affixed to either a mitegen mount and cooled to −173 °C. The crystals were then mounted on a Siemens three-circle goniometer platform equipped with an APEX detector. A graphite monochromator was employed for wavelength selection of the Mo KR radiation (λ) 0.71073 Å). The data were processed and refined using the program SAINT supplied by Siemens Industrial Automation Inc. Structures were solved direct methods and refined by standard difference Fourier techniques in the SHELXTL program suite (6.10 v., Sheldrick G. M., and Siemens Industrial Automation Inc., 2000). Hydrogen atoms were placed in calculated positions using the standard riding model and refined isotropically; all other atoms were refined anisotropically.

Table S1. Crystal Intensity Collection and Refinement Data

	trans-$[PNP^{Pr^i}]Ir(H)(Me)(CO)$	trans-$[PNP^{Pr^i}]Ir(H)(Et)(CO)$	$[PNP^{Pr^i}]Ir(N_2)\cdot MesNH_2$
lattice	Triclinic	Monoclinic	Triclinic
formula	$C_{28}H_{44}IrNOP_2$	$C_{29}H_{46}IrNOP_2$	$C_{35}H_{53}IrN_4P_2$
formula weight	664.78	678.81	783.95
space group	P–1	P2(1)/n	P–1
$a/Å$	8.3135(8)	14.7286(13)	9.8992(12)
$b/Å$	9.8060(10)	12.3197(11)	11.2251(14)
$c/Å$	17.8528(17)	16.0250(14)	16.388(2)
$\alpha/°$	84.829(2)	90.00	101.780(2)
$\beta/°$	83.244(2)	90.754(2)	93.376(2)
$\gamma/°$	75.962(2)	90.00	93.801(2)
$V/Å^3$	1399.3(2)	2907.5(4)	1773.9(4)
Z	2	4	2
temperature (K)	100	100	100
radiation (λ, Å)	0.71073	0.71073	0.71073
ρ (calcd), g cm^{-3}	1.578	1.551	1.468
μ (Mo K$_\alpha$), mm^{-1}	4.906	4.724	3.882
θ max, deg.	30.56	31.65	30.50
no. of data	8284	9217	10498
no. of parameters	304	313	384
R_1 (observed)	0.0471	0.0226	0.0535
wR_2 (observed)	0.0732	0.0529	0.0944
GOF	1.024	1.002	1.005
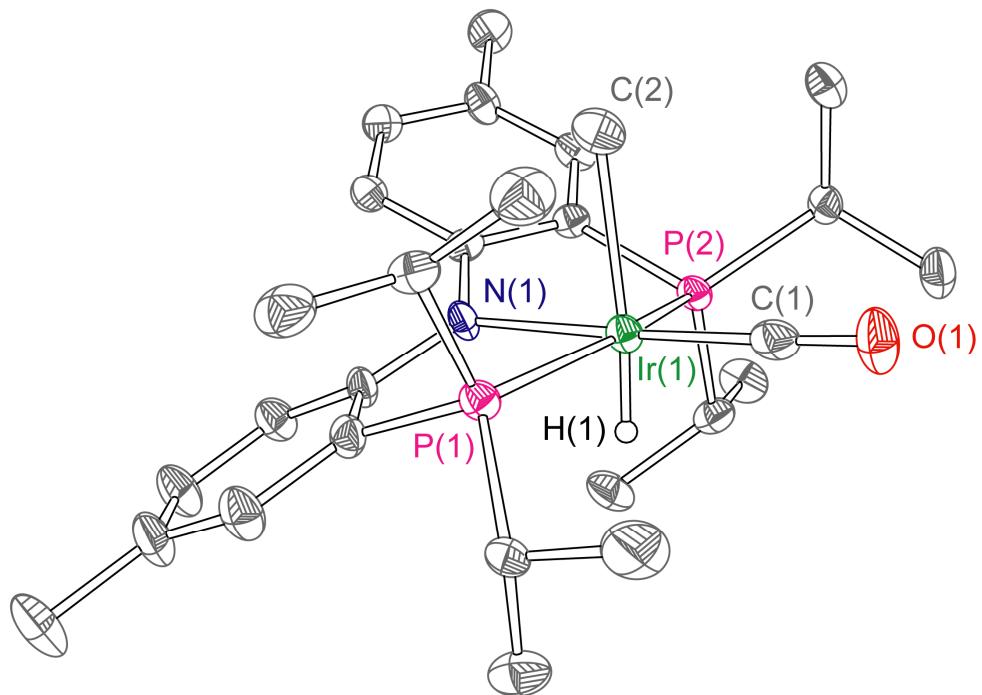
Figure S6. The molecular structure of *trans*-[PNP$^{Pr^i}$]Ir(H)(Me)(CO). Data collected at 100 K, thermal ellipsoids are drawn at the 50% probability level.
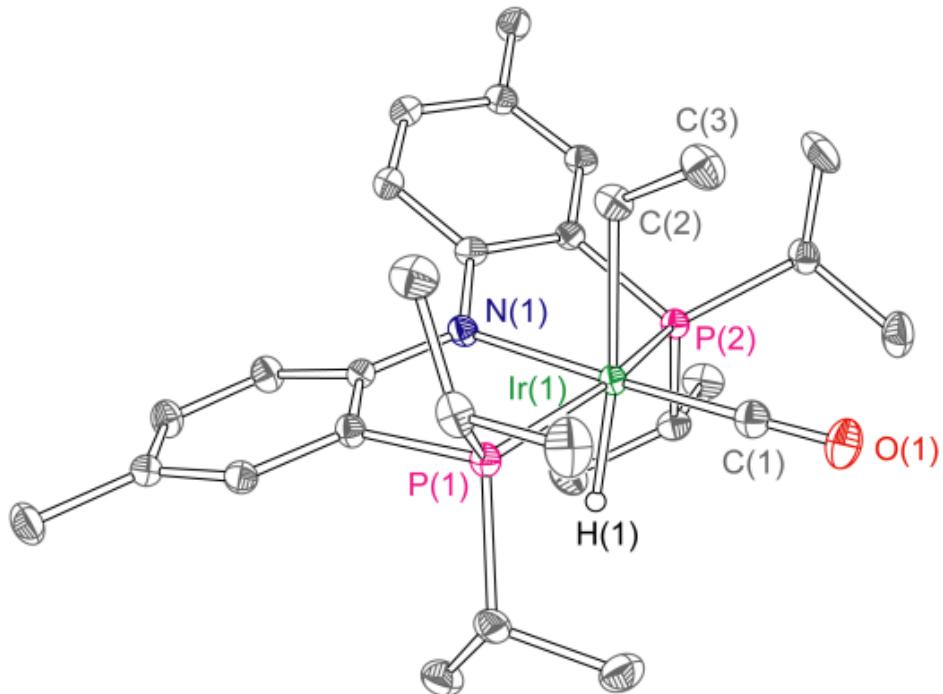
Figure S7. The molecular structure of *trans*-[PNP$^{Pr^i}$]Ir(H)(Et)(CO). Data collected at 100 K, thermal ellipsoids are drawn at the 50% probability level
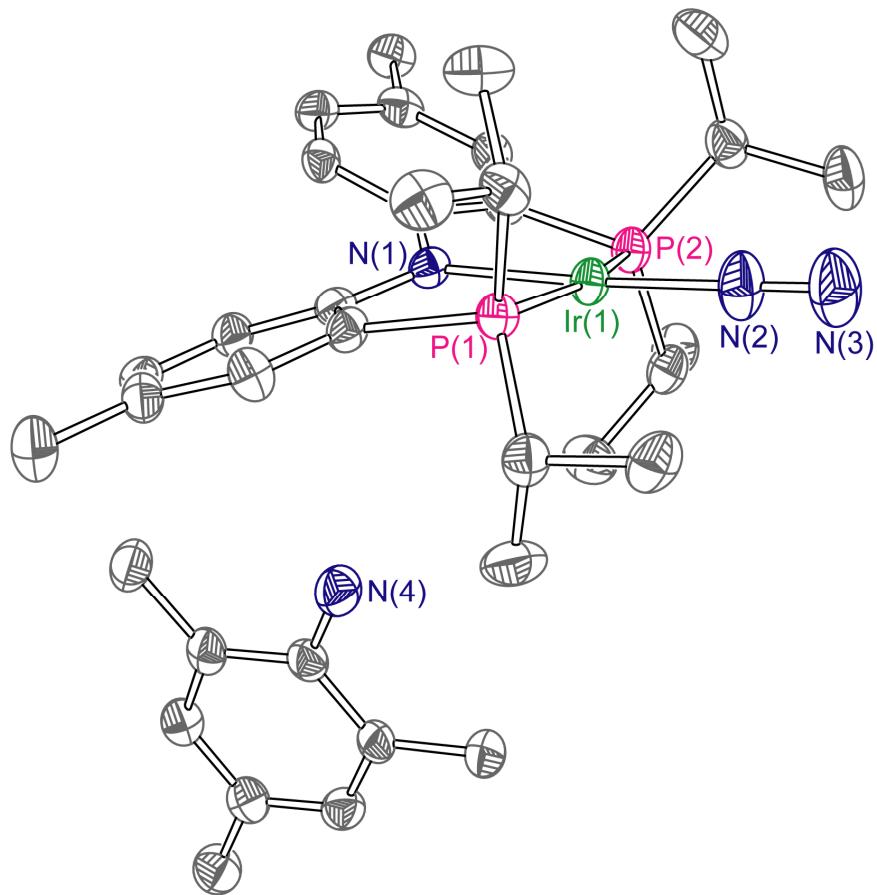
Figure S8. The molecular structure of $[PNP^{Pr^i}]Ir(N_2) \cdot MesNH_2$. Data collected at 100 K, thermal ellipsoids are drawn at the 50% probability level.

Computational Details. All calculations were carried out using DFT as implemented in the Gaussian03[6] suite of programs. Geometry optimizations were performed with the B3LYP density functional[7-10] and the 6-31G* (C, H, N, P, O). An effective core potential (ECP) representing the 1s2s2p3s3p3d4s4p4d core was used for the iridium atoms with a double-ζ basis set (LANL2DZ). All calculations were spin-restricted, and geometry optimizations proceeded without imposed symmetry. Minima were determined by the absence of imaginary frequencies in frequency calculations. Transition states were determined by one and only one imaginary frequency, which showed a mode of vibration along the bond that is cleaved. Comparison of bond lengths in the calculated structures to analogous metrics in single-crystal X-ray diffraction data show close agreement. X-ray *trans*-[PNP$^{Pr^i}$]Ir(H)(Me)(CO) Ir–P = 2.32 Å, 2.32 Å; Ir–N = 2.10 Å. Calculated [PNP$^{Pr^i}$]Ir(H)(OEt). Ir–P = 2.35 Å, 2.36 Å; Ir–N = 2.12 Å. Calculated [PNP^{Pri}]Ir(H)(CH(OH)Me) Ir–P = 2.36 Å, 2.33 Å; Ir–N = 2.11 Å.

[6]   Gaussian 03, Revision C.02, Frisch, M. J.; Trucks, G. W.; Schlegel, H. B.; Scuseria, G. E.; Robb, M. A.; Cheeseman, J. R.; Montgomery, Jr., J. A.; Vreven, T.; Kudin, K. N.; Burant, J. C.; Millam, J. M.; Iyengar, S. S.; Tomasi, J.; Barone, V.; Mennucci, B.; Cossi, M.; Scalmani, G.; Rega, N.; Petersson, G. A.; Nakatsuji, H.; Hada, M.; Ehara, M.; Toyota, K.; Fukuda, R.; Hasegawa, J.; Ishida, M.; Nakajima, T.; Honda, Y.; Kitao, O.; Nakai, H.; Klene, M.; Li, X.; Knox, J. E.; Hratchian, H. P.; Cross, J. B.; Bakken, V.; Adamo, C.; Jaramillo, J.; Gomperts, R.; Stratmann, R. E.; Yazyev, O.; Austin, A. J.; Cammi, R.; Pomelli, C.; Ochterski, J. W.; Ayala, P. Y.; Morokuma, K.; Voth, G. A.; Salvador, P.; Dannenberg, J. J.; Zakrzewski, V. G.; Dapprich, S.; Daniels, A. D.; Strain, M. C.; Farkas, O.; Malick, D. K.; Rabuck, A. D.; Raghavachari, K.; Foresman, J. B.; Ortiz, J. V.; Cui, Q.; Baboul, A. G.; Clifford, S.; Cioslowski, J.; Stefanov, B. B.; Liu, G.; Liashenko, A.; Piskorz, P.; Komaromi, I.; Martin, R. L.; Fox, D. J.; Keith, T.; Al-Laham, M. A.; Peng, C. Y.; Nanayakkara, A.; Challacombe, M.; Gill, P. M. W.; Johnson, B.; Chen, W.; Wong, M. W.; Gonzalez, C.; and Pople, J. A.; Gaussian, Inc., Wallingford CT, 2004.
[7]   (a) Becke, A. D. *J. Chem. Phys.* **1993**, *98*, 5648-5652. (b) Becke, A. D. *Phys. Rev. A* **1988**, *38*, 3098-3100.
[8]   Lee, C. T.; Yang, W. T.; Parr, R. G. *Phys. Rev. B* **1988**, *37*, 785-789.
[9]   Vosko, S. H.; Wilk, L.; Nusair, M. *Can. J. Phys.* **1980**, *58*, 1200-1211.
[10] Slater, J. C. *Quantum Theory of Molecules and Solids, Vol. 4: The Self-Consistent Field for Molecules and Solids*; McGraw-Hill: New York, 1974.
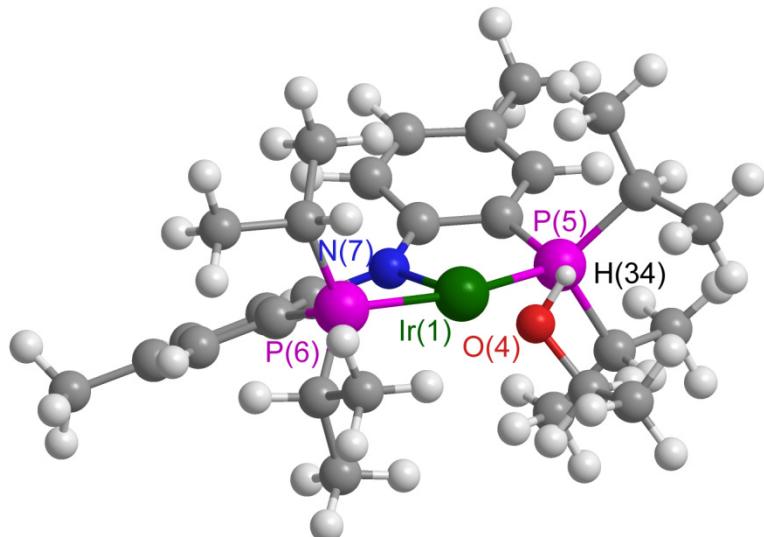
Figure S9. Geometry optimized structure of the starting materials of ethanol decarbonylation, [PNP$^{Pr^i}$]Ir and EtOH.
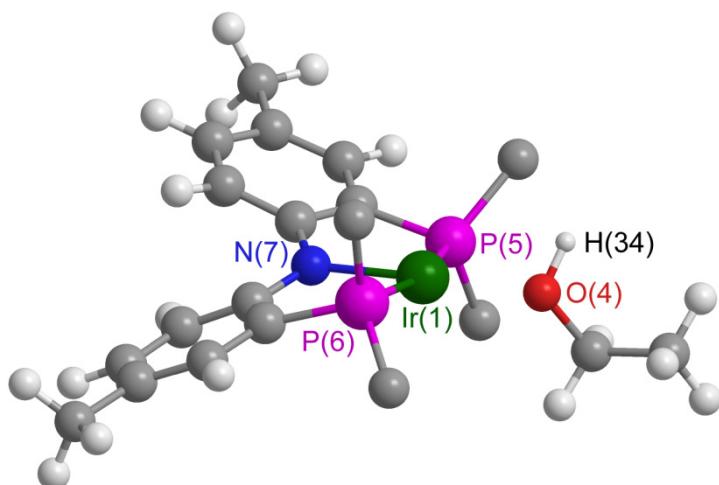
Figure S10. Geometry optimized structure of the starting materials of ethanol decarbonylation, [PNP$^{Pr^i}$]Ir and EtOH. (methyl groups of ligand isopropyl groups omitted for clarity).
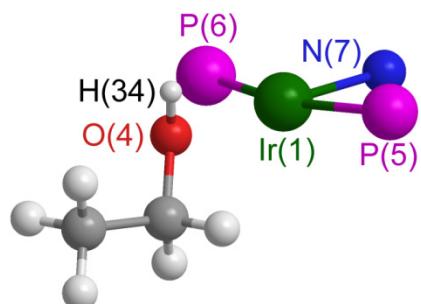
Figure S11. Coordination sphere of the geometry optimized structure of the starting materials of ethanol decarbonylation, [PNP$^{Pr^i}$]Ir and EtOH.
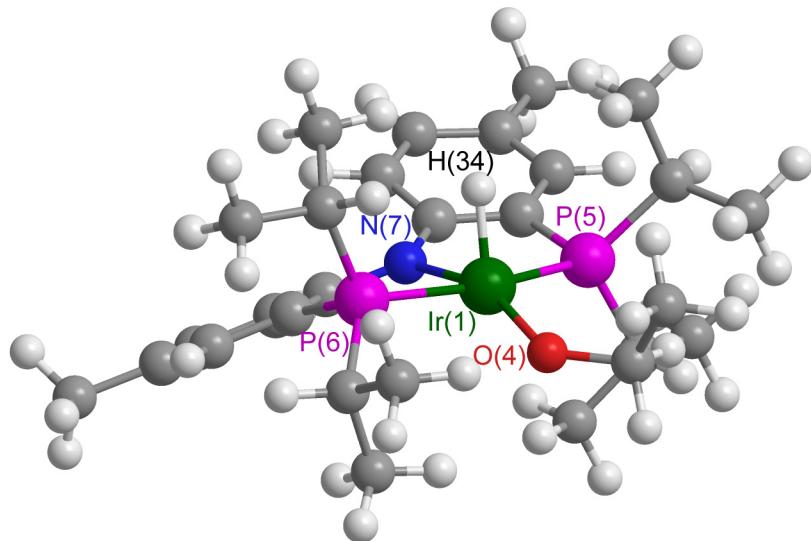
Figure S12. Geometry optimized structure of [PNP$^{Pr^i}$]Ir(H)(OEt).
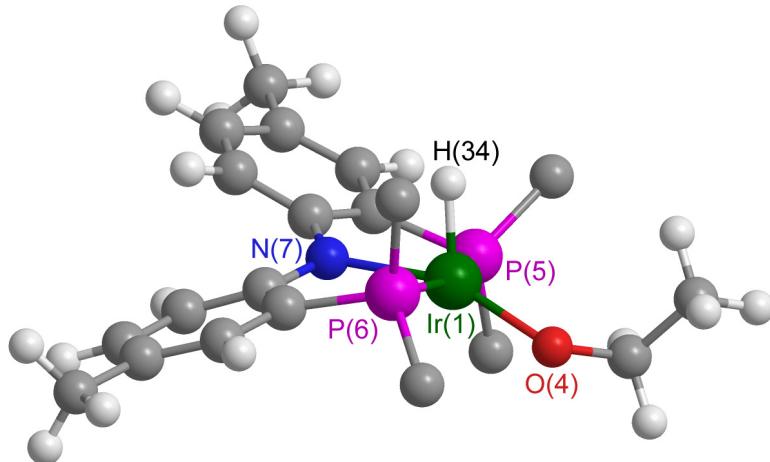
Figure S13. Geometry optimized structure of [PNP$^{Pr^i}$]Ir(H)(OEt) (methyl groups of ligand isopropyl groups omitted for clarity).
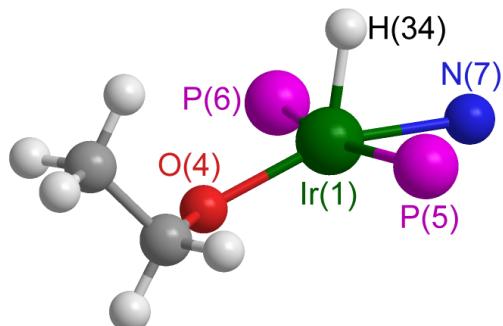
Figure S14. Coordination sphere of the geometry optimized structure of [PNP$^{Pr^i}$]Ir(H)(OEt).
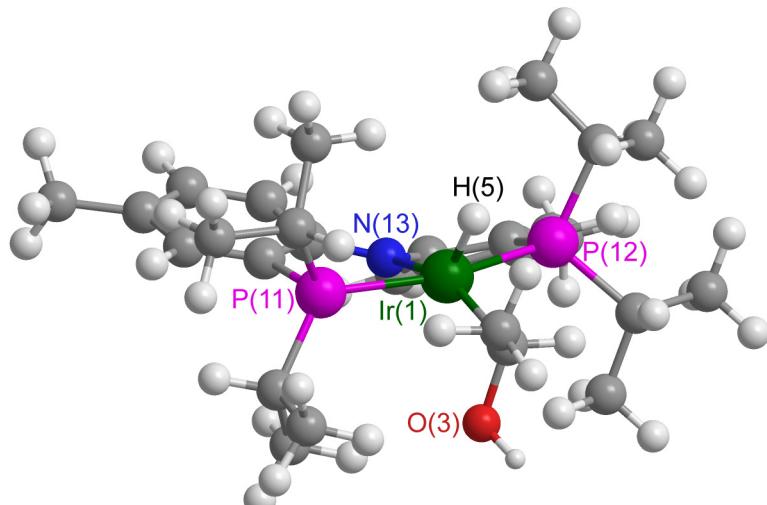
Figure S15. Geometry optimized structure of [PNP^{Pri}]Ir(H)(CH(OH)Me).
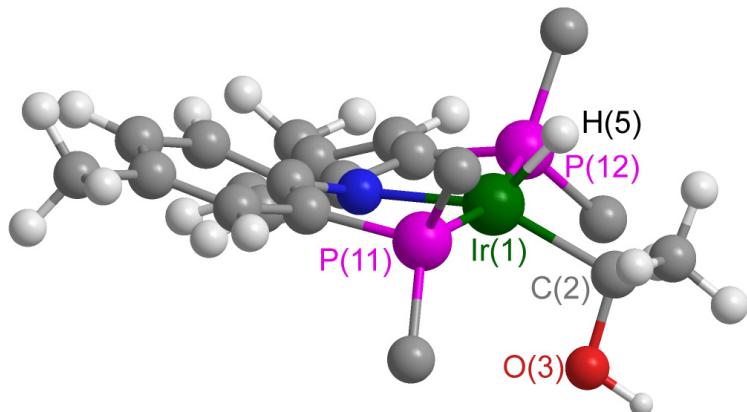
Figure S16. Geometry optimized structure of [PNP^{Pri}]Ir(H)(CH(OH)Me) (methyl groups of ligand isopropyl groups omitted for clarity).
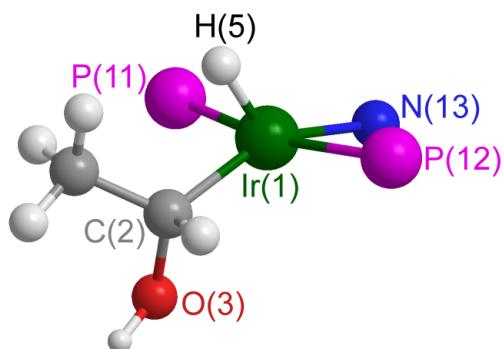
Figure S17. Coordination sphere of the geometry optimized structure of [PNP^{Pri}]Ir(H)(CH(OH)Me).
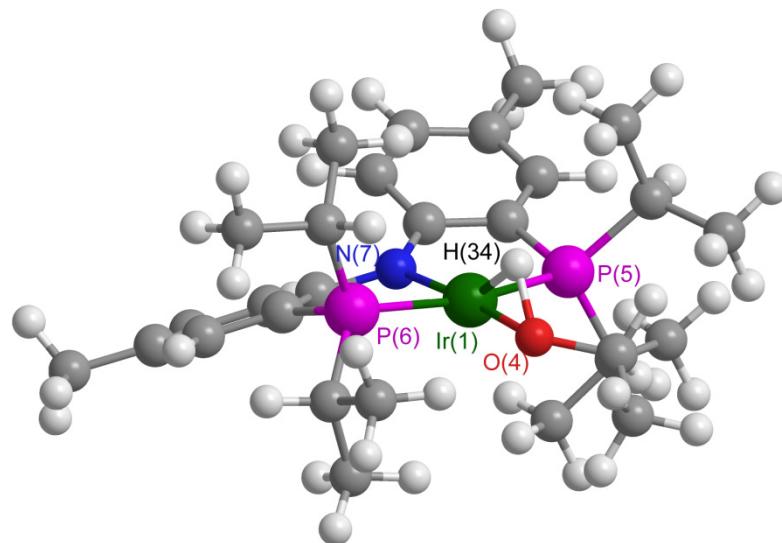
Figure S18. Calculated transition state of OH oxidative addition of EtOH to [PNP$^{Pr^i}$]Ir.
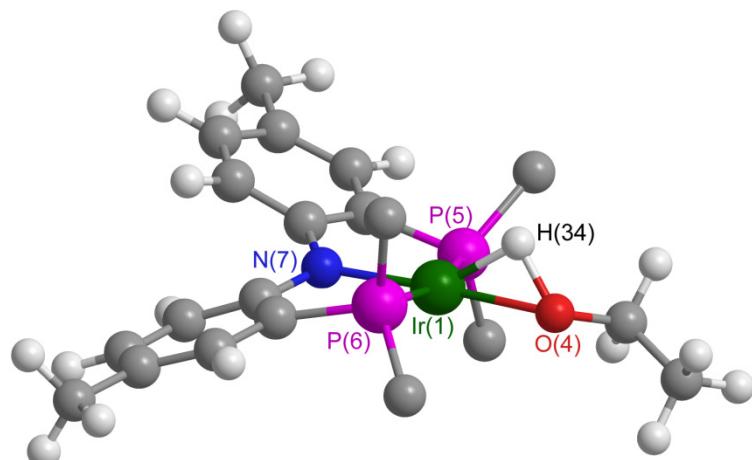
Figure S19. Calculated transition state of OH oxidative addition of EtOH to [PNP$^{Pr^i}$]Ir. (methyl groups of ligand isopropyl groups omitted for clarity).
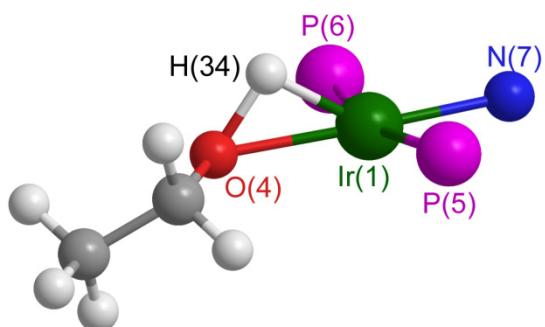
Figure S20. Coordination sphere of the calculated transition state of OH oxidative addition of EtOH to [PNP$^{Pr^i}$]Ir.
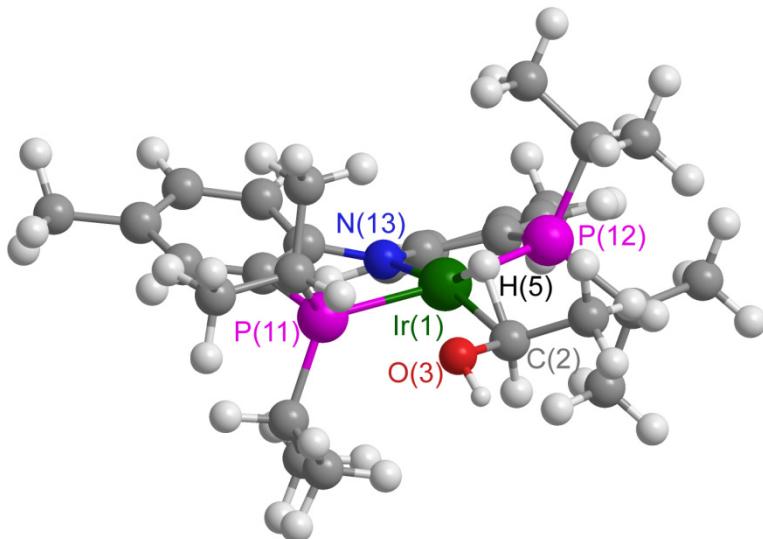
Figure S21. Calculated transition state of methylene CH oxidative addition of EtOH to [PNP$^{Pr^i}$]Ir.
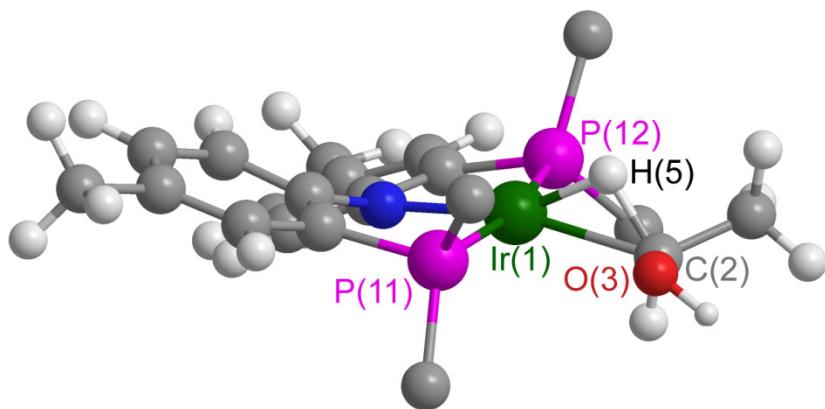
Figure S22. Calculated transition state of methylene CH oxidative addition of EtOH to [PNP$^{Pr^i}$]Ir. (methyl groups of ligand isopropyl groups omitted for clarity).
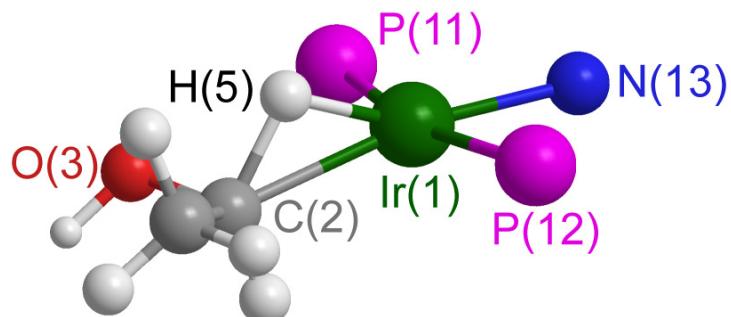
Figure S23. Coordination sphere of the calculated transition state of methylene CH oxidative addition of EtOH to [PNP$^{Pr^i}$]Ir.

Table S3. Cartesian Coordinates for the Geometry Optimized structure of EtOH and [PNP$^{Pr^i}$]Ir (E = −2012.1324467 Hartrees, E$_{rel}$ = 0 kcal/mol).

Atom	x	y	z
Ir1	−0.00481	−0.789223	0.073124
C2	0.364525	−3.80847	−0.926826
C3	0.22177	−5.294596	−0.634932
O4	−0.054895	−3.013539	0.208054
P5	2.264605	−0.46751	−0.233982
P6	−2.266633	−0.49528	0.455054
N7	−0.040486	1.264528	−0.063695
C8	2.381722	1.325274	0.067903
C9	1.125458	1.986698	0.165209
C10	1.158441	3.34368	0.580619
C11	2.356963	4.004996	0.803517
C12	3.602174	3.37302	0.644406
C13	3.577378	2.022679	0.293413
C14	4.897562	4.117709	0.865974
C15	−2.468082	1.209798	−0.158349
C16	−1.241342	1.89062	−0.395527
C17	−1.332899	3.1467	−1.047584
C18	−2.560415	3.710044	−1.366862
C19	−3.776215	3.069722	−1.075415
C20	−3.693189	1.808248	−0.482824
C21	−5.103649	3.70765	−1.411412
C22	3.531977	−1.212522	0.950021
C23	3.146169	−0.910101	2.406506
C24	2.991144	−0.789764	−1.951109
C25	2.080722	−0.13596	−3.003786
C26	4.456611	−0.378675	−2.155334
C27	−3.570361	−1.505945	−0.45116
C28	−3.645082	−2.938359	0.103146
C29	−3.289041	−1.503947	−1.96153
C30	−2.84344	−0.508256	2.254751
C31	−4.308397	−0.101891	2.472736
C32	−1.897756	0.359057	3.101045
C33	3.705364	−2.722875	0.730482
H34	0.511563	−3.213578	0.971413
H35	1.393021	−3.544678	−1.197282

H36	−0.289668	−3.487547	−1.738144
H37	−0.811291	−5.545707	−0.373934
H38	0.87227	−5.605623	0.19233
H39	0.507592	−5.878227	−1.517475
H40	0.228466	3.868576	0.76349
H41	2.325602	5.042474	1.13299
H42	4.523514	1.491079	0.216851
H43	5.750559	3.43111	0.904878
H44	4.884976	4.684472	1.805815
H45	5.097415	4.839954	0.062073
H46	−0.426807	3.664958	−1.338672
H47	−2.574437	4.670569	−1.879808
H48	−4.615826	1.264103	−0.291209
H49	−5.135467	4.057379	−2.451435
H50	−5.310852	4.579982	−0.776197
H51	−5.930265	3.001718	−1.274525
H52	4.495021	−0.728435	0.741668
H53	3.885737	−1.343714	3.092473
H54	2.16215	−1.330258	2.645747
H55	3.096954	0.166164	2.593818
H56	2.917812	−1.880203	−2.073991
H57	2.406091	−0.414526	−4.014509
H58	2.118688	0.956785	−2.927346
H59	1.038339	−0.441402	−2.866431
H60	4.777839	−0.634761	−3.173486
H61	5.139442	−0.882099	−1.461834
H62	4.582517	0.70241	−2.034253
H63	−4.541083	−1.021175	−0.283512
H64	−4.370538	−3.527482	−0.472451
H65	−3.961589	−2.961254	1.151509
H66	−2.672577	−3.438124	0.036744
H67	−4.055556	−2.085904	−2.489905
H68	−2.309739	−1.94586	−2.177802
H69	−3.289573	−0.488729	−2.369462
H70	−2.717372	−1.553742	2.56972
H71	−4.556212	−0.154517	3.540905
H72	−5.011862	−0.752006	1.941073
H73	−4.482406	0.928866	2.145158
H74	−2.154834	0.270943	4.164724
H75	−1.980639	1.41601	2.822348

H76	−0.855176	0.057761	2.959179
H77	4.46017	−3.123832	1.418406
H78	4.022563	−2.968741	−0.288652
H79	2.77012	−3.261761	0.931329

Table S4. Cartesian Coordinates for Geometry Optimized Structures [PNP$^{Pr^i}$]Ir(H)(CH(OH)Me) (E = −2012.1275112 Hartrees, E$_{rel}$ = +3.1 kcal/mol).

Atom	x	y	z
Ir1	0.009434	−0.880275	0.080566
C2	0.096974	−2.861677	−0.634996
O3	−0.208304	−2.718461	−2.04657
C4	−0.767646	−3.962612	−0.021322
H5	−0.112361	−1.79259	1.353002
H6	1.141342	−3.20047	−0.558806
H7	0.002657	−3.562646	−2.486038
H8	−0.662232	−4.91029	−0.5769
H9	−1.829586	−3.700152	−0.020726
H10	−0.466176	−4.152379	1.015782
P11	−2.306679	−0.520795	−0.145074
P12	2.289885	−0.598125	0.462294
N13	0.070231	1.218677	−0.141237
C14	−2.360289	1.306892	−0.010113
C15	−1.101058	1.965403	0.052996
C16	−1.130819	3.33947	0.394803
H17	−0.202724	3.867858	0.573129
C18	−2.327607	4.031778	0.533975
H19	−2.290962	5.087215	0.798896
C20	−3.570546	3.412902	0.343676
C21	−3.550574	2.039017	0.09106
H22	−4.499371	1.521606	−0.021508
C23	−4.863109	4.190813	0.421007
H24	−5.725815	3.523901	0.526806
H25	−5.028627	4.795944	−0.481185
H26	−4.869017	4.881139	1.273466
C27	2.505315	1.156725	−0.007178
C28	1.309351	1.836125	−0.369969
C29	1.470246	3.085775	−1.016026
H30	0.601415	3.591142	−1.420638
C31	2.719741	3.674967	−1.161444
H32	2.787438	4.637647	−1.665496
C33	3.889241	3.06615	−0.68135
C34	3.74893	1.793151	−0.124688
H35	4.640857	1.276676	0.219132

C36	5.235342	3.742009	−0.79734
H37	5.482671	3.979816	−1.840214
H38	6.035352	3.104627	−0.405645
H39	5.265208	4.687175	−0.239279
C40	−3.357969	−1.214559	1.261793
H41	−3.13628	−2.288661	1.21374
C42	−2.849305	−0.687323	2.614036
H43	−3.367723	−1.20183	3.433009
H44	−3.043362	0.386174	2.714121
H45	−1.773878	−0.849265	2.729359
C46	−4.881875	−1.037675	1.152799
H47	−5.370106	−1.622036	1.943207
H48	−5.287178	−1.379044	0.195511
H49	−5.176428	0.006439	1.297205
C50	−3.262838	−0.863023	−1.731088
H51	−4.218148	−0.334096	−1.607503
C52	−3.543586	−2.353648	−1.971624
H53	−4.169998	−2.467575	−2.865843
H54	−4.073191	−2.828445	−1.138054
H55	−2.604673	−2.886505	−2.139688
C56	−2.516734	−0.250636	−2.928531
H57	−3.119085	−0.369366	−3.838497
H58	−1.560066	−0.759307	−3.081016
H59	−2.327964	0.818382	−2.787279
C60	3.449097	−1.617481	−0.619816
H61	3.167777	−2.646917	−0.357697
C62	4.959027	−1.471325	−0.372615
H63	5.495283	−2.234985	−0.950533
H64	5.236775	−1.603889	0.678288
H65	5.329313	−0.497197	−0.705601
C66	3.105169	−1.401509	−2.104449
H67	3.718547	−2.067285	−2.72539
H68	3.318543	−0.371304	−2.410609
H69	2.051589	−1.612451	−2.312568
C70	2.949294	−0.772662	2.209973
H71	3.987365	−0.413231	2.185485
C72	2.940316	−2.238648	2.671105
H73	3.330851	−2.311747	3.693751
H74	3.557577	−2.882931	2.035659
H75	1.920748	−2.639979	2.671624

C76	2.153046	0.120433	3.174224
H77	2.581825	0.055095	4.18225
H78	1.105653	−0.194979	3.225965
H79	2.173635	1.169628	2.863315

Table S5. Cartesian Coordinates for Geometry Optimized Structures [PNP$^{Pr^i}$]Ir(H)(OEt) (E = −2012.146217 Hartrees E$_{rel}$ = −8.6 kcal/mol)

Atom	x	y	z
Ir1	−0.012574	−0.843644	0.039283
C2	0.641852	−3.71562	−0.851954
C3	0.68569	−4.709194	0.310516
O4	−0.299979	−2.70276	−0.628138
P5	2.292624	−0.457523	−0.269295
P6	−2.311549	−0.570093	0.417946
N7	−0.064032	1.271223	0.010119
C8	2.357422	1.328332	0.115013
C9	1.100508	1.982649	0.251389
C10	1.130642	3.323138	0.717545
C11	2.326209	3.984469	0.950387
C12	3.571912	3.365656	0.750334
C13	3.551119	2.029737	0.350962
C14	4.865894	4.109862	0.981368
C15	−2.49114	1.157407	−0.127802
C16	−1.273231	1.877123	−0.305131
C17	−1.386048	3.162211	−0.898888
C18	−2.619244	3.712672	−1.212842
C19	−3.826216	3.032074	−0.977287
C20	−3.724473	1.745821	−0.448955
C21	−5.16096	3.65779	−1.306087
C22	3.604171	−1.195837	0.864159
C23	3.179497	−1.062778	2.335279
C24	2.958139	−0.682646	−2.018412
C25	1.979976	−0.046501	−3.02021
C26	4.389652	−0.174006	−2.245654
C27	−3.514507	−1.589084	−0.594721
C28	−3.547622	−3.045057	−0.096862
C29	−3.143554	−1.525278	−2.085446
C30	−2.9337	−0.683417	2.193072
C31	−4.447678	−0.45775	2.343649
C32	−2.157521	0.278115	3.106897
C33	3.973047	−2.648322	0.528352
H34	0.258798	−0.515579	1.543758
H35	1.650332	−3.308177	−1.027748

H36	0.353307	–4.252229	–1.771761
H37	–0.300038	–5.163654	0.460521
H38	0.962392	–4.196934	1.239587
H39	1.410829	–5.512064	0.12274
H40	0.198219	3.832104	0.93078
H41	2.2932	5.008443	1.31896
H42	4.502072	1.514875	0.238416
H43	5.725085	3.43046	0.967798
H44	4.868075	4.628331	1.948557
H45	5.040747	4.873045	0.210582
H46	–0.487992	3.714826	–1.147875
H47	–2.645786	4.697291	–1.676976
H48	–4.63672	1.170759	–0.305867
H49	–5.176965	4.068362	–2.323705
H50	–5.402661	4.485164	–0.62483
H51	–5.972847	2.926203	–1.231418
H52	4.498452	–0.578351	0.711351
H53	3.990385	–1.408044	2.988909
H54	2.293364	–1.672375	2.54281
H55	2.948735	–0.026522	2.600376
H56	2.943294	–1.769703	–2.174135
H57	2.317952	–0.236198	–4.046547
H58	1.921628	1.038779	–2.880137
H59	0.969835	–0.454439	–2.912233
H60	4.69985	–0.391212	–3.275637
H61	5.118059	–0.647281	–1.578266
H62	4.449949	0.910215	–2.104818
H63	–4.507776	–1.13976	–0.461679
H64	–4.238893	–3.63064	–0.716214
H65	–3.888523	–3.126163	0.94115
H66	–2.54978	–3.485796	–0.174195
H67	–3.891036	–2.071359	–2.674918
H68	–2.166986	–1.989593	–2.252474
H69	–3.110539	–0.494854	–2.454061
H70	–2.697689	–1.713044	2.493857
H71	–4.732839	–0.571601	3.397043
H72	–5.043694	–1.169773	1.764391
H73	–4.728331	0.555864	2.036673
H74	–2.496383	0.157583	4.143321
H75	–2.328481	1.320747	2.816139

H76	−1.080729	0.092822	3.076119
H77	4.80033	−2.972091	1.172332
H78	4.297409	−2.77361	−0.509921
H79	3.133483	−3.325897	0.706924

Table S6. Cartesian Coordinates for Transition State of CH oxidative addition of EtOH to [PNP$^{Pr^i}$]Ir (E = –2012.1022493 Hartrees, E_{rel} = +18.9 kcal/mol, imaginary frequency = 681.53i cm^{-1}).

Atom	x	y	z
Ir1	–0.007217	–0.835932	0.019024
C2	–0.124063	–3.108514	–0.386043
O3	–1.483258	–3.561437	–0.324498
C4	0.79742	–4.191813	0.180467
H5	–0.142671	–2.299128	0.754447
H6	0.15821	–2.888299	–1.423292
H7	–1.537333	–4.385218	–0.837625
H8	0.702069	–5.113757	–0.411749
H9	0.535337	–4.430725	1.217255
H10	1.846842	–3.889973	0.150782
P11	–2.297384	–0.489875	–0.290177
P12	2.282632	–0.572969	0.366191
N13	0.044715	1.22509	–0.084553
C14	–2.383862	1.303607	0.044758
C15	–1.124373	1.945698	0.185755
C16	–1.147756	3.278334	0.666626
H17	–0.216718	3.781204	0.898094
C18	–2.34268	3.954841	0.873361
H19	–2.304612	4.976346	1.248481
C20	–3.588542	3.361296	0.61988
C21	–3.573181	2.023122	0.221177
H22	–4.5225	1.522619	0.051695
C23	–4.878488	4.128947	0.789377
H24	–5.745372	3.459088	0.784105
H25	–5.027603	4.86104	–0.016464
H26	–4.896217	4.687295	1.733819
C27	2.476507	1.1974	–0.033974
C28	1.260125	1.875073	–0.31139
C29	1.374789	3.171793	–0.873275
H30	0.482602	3.688102	–1.20765
C31	2.607678	3.790579	–1.022993
H32	2.641783	4.786294	–1.462249
C33	3.80535	3.170338	–0.630474
C34	3.705484	1.862131	–0.154621

H35	4.61679	1.341705	0.126615
C36	5.133959	3.880519	−0.741421
H37	5.278094	4.318524	−1.737416
H38	5.968802	3.195569	−0.557025
H39	5.219274	4.702142	−0.017097
C40	−3.439954	−1.367051	0.924085
H41	−3.18545	−2.416596	0.743127
C42	−3.029772	−1.022889	2.366135
H43	−3.588429	−1.651242	3.071769
H44	−3.245952	0.024697	2.604017
H45	−1.959615	−1.191502	2.524025
C46	−4.954405	−1.192222	0.725182
H47	−5.487269	−1.881163	1.393514
H48	−5.280408	−1.413665	−0.29623
H49	−5.286501	−0.180376	0.978059
C50	−3.101901	−0.649217	−1.98848
H51	−4.08611	−0.170618	−1.887239
C52	−3.311804	−2.096055	−2.458404
H53	−3.851504	−2.094513	−3.414387
H54	−3.89003	−2.691544	−1.745577
H55	−2.354296	−2.603086	−2.611552
C56	−2.286965	0.145404	−3.022105
H57	−2.777769	0.098064	−4.002713
H58	−1.277619	−0.269048	−3.123242
H59	−2.19021	1.198321	−2.74123
C60	3.43094	−1.51299	−0.808532
H61	3.166418	−2.56184	−0.623091
C62	4.945944	−1.375722	−0.585732
H63	5.474934	−2.084211	−1.236336
H64	5.246863	−1.591895	0.444459
H65	5.30216	−0.374257	−0.843992
C66	3.059877	−1.18978	−2.266226
H67	3.62129	−1.839155	−2.950022
H68	3.302914	−0.150553	−2.512283
H69	1.99011	−1.333901	−2.450108
C70	3.034488	−0.779292	2.077518
H71	4.059451	−0.387752	2.018022
C72	3.089541	−2.250708	2.513668
H73	3.546431	−2.329913	3.508098
H74	3.679337	−2.872183	1.830626

H75	2.081827	−2.67571	2.57583
C76	2.249797	0.067382	3.092036
H77	2.700747	−0.027952	4.088101
H78	1.207427	−0.264028	3.150122
H79	2.249638	1.126844	2.818168

Table S7. Cartesian Coordinates for Transition State of OH oxidative addition of EtOH to [PNP$^{Pr^i}$]Ir (E = –2012.1092443 Hartrees, E$_{rel}$ = +14.6 kcal/mol, imaginary frequency = 1158.39i cm^{-1}).

Atom	x	y	z
Ir1	–0.025278	–0.795082	0.017305
C2	0.70328	–3.907574	–0.190052
C3	0.045656	–5.180784	–0.713251
O4	–0.313048	–2.967895	0.120955
P5	2.288704	–0.48201	–0.247456
P6	–2.296277	–0.503328	0.41277
N7	–0.036437	1.254844	–0.065719
C8	2.386464	1.317654	0.070391
C9	1.133004	1.974004	0.188828
C10	1.156108	3.314781	0.644733
C11	2.351647	3.98016	0.87749
C12	3.596871	3.361915	0.685384
C13	3.578226	2.019901	0.300941
C14	4.890654	4.109556	0.906695
C15	–2.475214	1.228326	–0.125409
C16	–1.244692	1.899098	–0.362868
C17	–1.327739	3.167952	–0.986871
C18	–2.552709	3.75636	–1.271766
C19	–3.77193	3.127415	–0.973794
C20	–3.697513	1.849857	–0.415721
C21	–5.095424	3.794337	–1.265656
C22	3.589309	–1.169982	0.933559
C23	3.114006	–1.019982	2.387344
C24	2.988344	–0.780889	–1.973525
C25	2.028752	–0.186355	–3.018006
C26	4.425349	–0.29006	–2.204677
C27	–3.555391	–1.483435	–0.572761
C28	–3.668171	–2.926189	–0.05162
C29	–3.178045	–1.460042	–2.062656
C30	–2.862164	–0.622113	2.202587
C31	–4.33486	–0.249009	2.430817
C32	–1.933942	0.20814	3.103441
C33	4.024207	–2.611783	0.634615
H34	0.024359	–2.104538	1.078623

H35	1.294008	–4.143643	0.709263
H36	1.394823	–3.509247	–0.945835
H37	–0.527491	–4.970968	–1.622681
H38	–0.638196	–5.596266	0.034797
H39	0.804553	–5.937969	–0.947636
H40	0.223067	3.827289	0.845657
H41	2.31582	5.007422	1.236341
H42	4.529634	1.503885	0.198556
H43	5.745292	3.42549	0.948452
H44	4.873801	4.678224	1.844825
H45	5.088653	4.829729	0.100784
H46	–0.419016	3.681258	–1.27827
H47	–2.561103	4.729093	–1.760754
H48	–4.623518	1.311408	–0.2262
H49	–5.117022	4.228035	–2.27322
H50	–5.303767	4.611823	–0.561693
H51	–5.925115	3.082819	–1.192613
H52	4.466797	–0.52618	0.796405
H53	3.911035	–1.327986	3.076089
H54	2.235359	–1.644983	2.579363
H55	2.844973	0.015033	2.619489
H56	2.968913	–1.874811	–2.07968
H57	2.379018	–0.423362	–4.030587
H58	1.976355	0.904827	–2.927706
H59	1.014918	–0.581831	–2.898643
H60	4.75307	–0.563635	–3.215845
H61	5.14192	–0.725148	–1.499657
H62	4.485838	0.800345	–2.123115
H63	–4.52585	–0.983913	–0.450261
H64	–4.355259	–3.49635	–0.689774
H65	–4.059492	–2.968689	0.970684
H66	–2.690787	–3.417857	–0.066765
H67	–3.938641	–1.991057	–2.649165
H68	–2.213525	–1.953657	–2.222069
H69	–3.105611	–0.437987	–2.448414
H70	–2.721607	–1.682967	2.45075
H71	–4.593039	–0.385567	3.488669
H72	–5.023267	–0.865158	1.842708
H73	–4.517122	0.801998	2.18132
H74	–2.210311	0.067374	4.156093

H75	−2.017026	1.277066	2.874997
H76	−0.887782	−0.083297	2.971909
H77	4.842859	−2.892465	1.309234
H78	4.385703	−2.739648	−0.390932
H79	3.208747	−3.320841	0.797551